

HEP'99 # 7.734  
Submitted to Pa 7  
Pl 7

DELPHI 99-97 CONF 284  
15 June 1999

# Interpretation of the searches for Higgs bosons in the MSSM with an additional scalar singlet

Preliminary

DELPHI Collaboration

OPEN-99-438  
15/06/1999



Paper submitted to the HEP'99 Conference  
Tampere, Finland, July 15-21



# Interpretation of the searches for Higgs bosons in the MSSM with an additional scalar singlet

Maarten Boonekamp, Vanina Ruhlmann-Kleider

CEA-Saclay, DSM/DAPNIA, France

## Abstract

The results of simplified analyses, designed to search for standard and non-minimal neutral Higgs boson production over a wide mass range, are described. The search for pair-produced  $h, A$  bosons relies mostly on b-quark tagging, while the search for Higgsstrahlung events also uses the signature of the on-shell Z boson in the final state.

Together with the latest published searches for charged Higgs bosons, these results are interpreted in the framework of an extended supersymmetric model, where an additional gauge-singlet Higgs field is introduced in the most general way. A pseudoscalar mass term,  $m'_A$ , which parameterizes this model, is found to be greater than  $69 \text{ GeV}/c^2$  for  $\tan\beta \geq 1$ , and greater than  $72 \text{ GeV}/c^2$  for large values of  $\tan\beta$ . For  $\tan\beta \leq 1$ , no limit can be set.

# 1 Introduction

Searches for non-standard neutral Higgs bosons are usually interpreted in the context of minimal supersymmetry [1], or in the more general non supersymmetric two Higgs doublet models [2]. The aim of the present work is to make a first step towards generalization of the Higgs boson search results within the supersymmetric scheme.

The model considered here is the MSSM extended by a gauge-singlet Higgs field in the most general CP-conserving way. This very general model has drawn modest attention in the literature, although a very extensive study was performed in preparation of LEP2 [3]. Its phenomenology is very close to that of the MSSM, with the notable difference that due to a large number of free parameters, the neutral Higgs boson mass spectrum is only loosely constrained. As a consequence, analyses covering a wide Higgs boson mass range are needed.

A Higgs singlet was first introduced to generate spontaneous parity breaking in the supersymmetric Standard Model [4], and is nowadays widely discussed as a potential solution to the supersymmetric  $\mu$ -problem [5]. This potential solution occurs in the so-called NMSSM or (M+1)SSM, a special case of the model discussed here, in which the Higgs superpotential is entirely trilinear and contains no dimensioned couplings. Having less freedom than the general model, a dedicated and more predictive interpretation could be performed; nevertheless, the NMSSM is included in our general analysis.

This article is organized as follows. The phenomenology of the model is briefly reviewed in the following section. The data collected by DELPHI near  $\sqrt{s} = 189$  GeV, representing  $158 \text{ pb}^{-1}$ , are analysed in the third section. The fourth section details the test of the parameter space, and the determination of the excluded regions. Finally conclusions, prospects and caveats are summarized in the last section.

## 2 The general MSSM plus a singlet

The extended Higgs potential arises from [3, 6]:

$$W = -\mu H_1 H_2 + \lambda N H_1 H_2 - \frac{\kappa}{3} N^3 + \frac{1}{2} \mu' N^2 + \mu'' N, \quad (1)$$

where the  $H_i$  are the Higgs doublets and  $N$  is the Higgs singlet. The vacuum expectation values  $v_1, v_2$  of the Higgs doublets are as usual expressed in terms of  $\tan \beta \equiv v_2/v_1$  and  $v^2 \equiv v_1^2 + v_2^2$ . Equation 1 represents the most general Higgs superpotential with this field content. When all dimensioned couplings (i.e.  $\mu, \mu', \mu''$ ) are set to 0, one obtains the NMSSM, whereas if all terms containing the singlet  $N$  are removed, the MSSM is recovered; in this sense, the present model is truly a generalization of the minimal supersymmetric model.

With respect to the MSSM, the singlet contributes two additional neutral Higgs bosons (one CP-even, the other CP-odd, corresponding to its real and imaginary components respectively), so that the spectrum contains seven Higgs bosons: five neutral bosons (two CP-odd, three CP-even) and two charged bosons. Their production modes at LEP are the usual  $e^+e^- \rightarrow hA, hZ$  and  $H^+H^-$  processes.

The neutral Higgs mass matrices are  $3 \times 3$ , and can be written as :

$$M_{odd}^2 = \begin{pmatrix} 0 & 0 & 0 \\ 0 & m_A'^2 & \cdot \\ 0 & \cdot & \cdot \end{pmatrix},$$

$$M_{even}^2 = \begin{pmatrix} m_Z^2 c_\beta^2 + m_A'^2 s_\beta^2 & -s_\beta c_\beta (m_Z^2 + m_A'^2 - 2\lambda^2 v^2) & \cdot \\ -s_\beta c_\beta (m_Z^2 + m_A'^2 - 2\lambda^2 v^2) & m_Z^2 s_\beta^2 + m_A'^2 c_\beta^2 & \cdot \\ \cdot & \cdot & \cdot \end{pmatrix}. \quad (2)$$

The CP-odd mass-matrix is given in a basis where the CP-odd Goldstone boson is already rotated away, leaving the physical combination of  $H_1$  and  $H_2$  that in turn mixes with the singlet. The CP-even mass-matrix is given in the basis  $(H_1, H_2, N)$ . The CP-odd mass parameter  $m_A'^2$  is the analog of  $m_A$  in the MSSM, but does not correspond to a physical mass in our case;  $\lambda$  is the trilinear doublet-singlet coupling parameter, and  $s_\beta$  and  $c_\beta$  are shorthands for  $\sin \beta$  and  $\cos \beta$ . The matrix entries represented by dots are related to terms of the Higgs potential involving the singlet field, which we are not attempting to specify: as explained below, they can be parameterized simply; in addition, they are scanned over in our interpretation, and do not appear in the results.

The CP-odd sector is determined after fixing two additional entries of its mass matrix, which we can parameterize as e.g. the mass of the lightest CP-odd Higgs bosons  $A_1$ , and the doublet-singlet mixing angle in the CP-odd sector. The mass of the heaviest CP-odd boson  $A_2$  is then determined by:

$$m_A'^2 = m_{A_1}^2 c_\gamma^2 + m_{A_2}^2 s_\gamma^2, \quad (3)$$

where the CP-odd mixing angle  $\gamma$  diagonalizes  $M_{odd}^2$ :

$$UM_{odd}^2 U^\dagger = \text{diag}(m_{A_1}^2, m_{A_2}^2).$$

The mass of the lightest CP-odd boson satisfies the bound  $m_{A_1} < m_A'$ .

The CP-even matrix contains three unknown entries and its diagonalization doesn't have a simple analytical expression. We will simply call  $V$  the matrix that exhibits the physical particles  $h_1$ ,  $h_2$  and  $h_3$  (ordered by increasing mass):

$$VM_{even}^2 V^\dagger = \text{diag}(m_{h_1}^2, m_{h_2}^2, m_{h_3}^2). \quad (4)$$

The lightest CP-even boson mass satisfies the following bound at tree level:

$$m_{h_1}^2 < \Lambda^2 \equiv m_Z^2 \cos^2 2\beta + \lambda^2 v^2 \sin^2 2\beta. \quad (5)$$

As in the MSSM, due to the mixing in the Higgs sector, the couplings of the neutral Higgs bosons to gauge bosons and fermions deviate from their Standard Model value by factors which we will note  $R_{h_i A_j}$ ,  $R_{h_i Z}$ ,  $R_{h_i u \bar{u}}$ ,  $R_{h_i d \bar{d}}$ ,  $R_{A_j u \bar{u}}$ ,  $R_{A_j d \bar{d}}$ . The  $R$  factors have expressions in terms of  $U$  and  $V$  matrix elements, and are given explicitly in [7]. We will just give a few examples, to illustrate the link with the MSSM. The  $R_{h_i Z}$  are given by:

$$R_{h_i Z} = c_\beta V_{i1} + s_\beta V_{i2}.$$

When the singlet does not mix with the doublets,  $V$  is just a rotation of the  $(H_1, H_2)$  basis, and one obtains, if  $V$  is a rotation of angle  $\alpha$ :

$$\begin{aligned} R_{h_1 Z} &= c_\beta (-s_\alpha) + s_\beta c_\alpha = \sin(\beta - \alpha), \\ R_{h_2 Z} &= c_\beta c_\alpha + s_\beta s_\alpha = \cos(\beta - \alpha), \\ R_{h_3 Z} &= 0; \end{aligned}$$

the MSSM relations are recovered for  $h_1$  and  $h_2$ , and  $h_3$  decouples. The  $R_{h_i Z}, m_{h_i}$  satisfy the sum rules:

$$\begin{aligned} R_{h_1 Z}^2 + R_{h_2 Z}^2 + R_{h_3 Z}^2 &= 1, \\ R_{h_1 Z}^2 m_{h_1}^2 + R_{h_2 Z}^2 m_{h_2}^2 + R_{h_3 Z}^2 m_{h_3}^2 &= \Lambda^2. \end{aligned} \tag{6}$$

The coupling factor of CP-odd bosons to up-type fermions,  $R_{A_j u \bar{u}}$ , are given by:

$$\begin{aligned} R_{A_1 u \bar{u}} &= \frac{U_{11}}{\tan \beta} = \frac{c_\gamma}{\tan \beta}, \\ R_{A_2 u \bar{u}} &= \frac{U_{21}}{\tan \beta} = \frac{s_\gamma}{\tan \beta}. \end{aligned}$$

When there is no singlet mixing in the CP-odd sector ( $c_\gamma=1$ ), the MSSM coupling is recovered for  $A_1$ , while  $A_2$  decouples.

It should be noted that for a given Higgs boson, its singlet component does affect its coupling to fermions, but not its branching fractions, which are identical to the MSSM ones (i.e. all couplings are diluted by the same amount due to singlet mixing, and the branching ratios deviate from their SM value due to Higgs doublet mixing only). In particular, one still expects the sufficiently heavy neutral Higgs boson to decay dominantly into  $b\bar{b}$ .

At tree level, the model is thus entirely specified by  $\tan \beta$ ,  $m'_A$ ,  $\lambda$ , and by five parameters related to singlet mixing (two parameters for the mixing in the CP-odd sector, and three parameters in the CP-even sector). As we have seen, CP-odd singlet mixing may be parameterized by one mass (one may take  $m_{A_1}$ , ranging from 0 to  $m'_A$ ) and one unconstrained mixing angle  $\gamma$ . Similarly, CP-even singlet mixing can be described by one mass (e.g.  $m_{h_1}$ , taking values between 0 and its bound Eq.5), one  $R_{h_i Z}$ -factor ranging from 0 to 1, and one remaining mixing angle [3].

Since the Higgs singlet field doesn't couple to any particles, except to other Higgs bosons, radiative corrections to the mass matrices of this model are very similar to those in the MSSM. They were computed in [3] following the method of [8]. Since all terms represented by dots in the matrices are considered unconstrained provided the matrices remain orthogonal, only the upper  $2 \times 2$  block of the CP-even matrix was corrected, bringing the usual Higgs bosons mass dependence on top and stop masses.

Also, the quartic term  $\lambda^2 |H_1 H_2|^2$  induced in the Higgs potential by the second term in Eq.1 is similar to the Standard Model quartic coupling, and the same perturbativity argument can be applied to set an upper bound on the value of  $\lambda$ : if the theory is to remain perturbative up to the grand unification scale, the value of  $\lambda$  at the electroweak scale can not exceed 0.6-0.7 (the uncertainty arises from the errors on  $\alpha_s$  and  $m_t$ ). This

condition, transmitted to the bound (5) modified by radiative corrections, sets an upper limit on the lightest CP-even Higgs boson mass of about 135-140 GeV/c<sup>2</sup> [3].

Finally, the expression of the charged Higgs boson mass in this model differs significantly from its MSSM counterpart. It reads, at tree level:

$$m_{H^\pm}^2 = m_W^2 + m_A'^2 - \lambda^2 v^2. \quad (7)$$

Radiative corrections to this relation are taken into account in our analysis, and have some impact at high values of  $\tan\beta$ . This relation implies that charged Higgs bosons at non-zero values of  $\lambda$  may well be within the LEP2 range, so that searches will provide a powerful test of the model.

### 3 Search strategy and analysis results

As we have seen in the previous section, after the addition of a Higgs singlet to the MSSM, large parts of predictivity are lost; in particular, the mass spectrum of the Higgs bosons is much less constrained than in the MSSM. For any value of  $m_A'$ ,  $\tan\beta$ , and  $\lambda$ , the lightest CP-even and odd neutral Higgs bosons can have arbitrary mass (up to their upper bounds Eqs. 3 and 5) and coupling factor. In consequence, there are always parameter configurations for which the experimental sensitivity to a given Higgs boson vanishes, and the search for a given neutral Higgs boson does not provide a full test of the model. Instead, one must rely on the contributions of all accessible Higgs bosons to the total Higgs production cross-section, since the sum of coupling factors amounts to the Standard Model value, as is shown for example in Eq.6.

A thorough test of the model would therefore require searches over the whole Higgs mass range accessible at LEP2, generating many different final states. Such a study has been performed on LEP1 data [9], and has not been updated yet. We restrain ourselves here to configurations where all Higgs bosons are heavier than 12 GeV/c<sup>2</sup>, so that the  $b\bar{b}$  decay is always open, and perform searches for the  $h_i Z$  and  $h_i A_j$  processes loosely dependent on kinematics above this threshold. Because they represent the largest branching ratio, only fully hadronic final states are considered. The data, methods and variables used for the present searches are a subset of those used in standard DELPHI Higgs analyses, and are described in the corresponding DELPHI papers [10]. Therefore, we will here only outline the selections and stress the main points (all details can however be found in [11]).

Multi-hadronic non radiative events are selected in a first stage. The hadronic preselection, and the rejection of events with initial state radiation proceed along the same lines as in [10]. Events are required to have high multiplicity and large total reconstructed energy. Events with energetic isolated charged particles are also rejected. Initial state photons are detected as energetic clusters in the calorimeters, or as large missing momentum along the beam line, and the events are required not to contain any such photon. The  $h_i A_j$  search is then based on the presence of four b-quarks in the final state, and in the  $h_i Z$  case, events are searched containing two b-quarks recoiling against an on-shell Z.

Since we are looking for events with four quarks in the final state, all selected events are reconstructed in four jets of particles using the Durham algorithm [12]. The b-quark content of each jet is evaluated using the DELPHI b-tagging algorithm [13]. The final

Analysis	$\epsilon(h_i A_j)$	$\epsilon(h_i Z)$	exp. background	data
4b	42.2%		$4.4 \pm 0.5$	2
2b-Z	40.3%	28.7%	$20.1 \pm 1.1$	26

Table 1: Signal efficiencies, expected background rates, and observed data for the mass independent Higgs searches. The result of the  $h_i Z$  analysis applied to the  $h_i A_j$  process is also shown.

$h_i A_j$  selection is then based on a global variable  $X_{hA}$  constructed from the four jet b-quark content variables, combined together with a likelihood ratio method. For the  $h_i Z$  selection, the six possibilities to reconstruct from four jets a Z recoiling against a Higgs boson are considered. In each case, the probability that the Higgs boson candidate dijet is a  $b\bar{b}$  pair is computed from the jet b-tagging variables, and the probability that the opposite dijet represents a Z boson decay is evaluated by performing a kinematic fit constraining its mass to be equal to the nominal Z mass, and taking the  $\chi^2$  probability of the fit. The dijet pairing is chosen to maximise the product of the b-tagging and  $\chi^2$  probabilities, and this maximum value is then used as a discriminating variable  $X_{hZ}$ . The final step consists of a selection based on these variables. The distributions of these variables for background, data and signal are illustrated in figure 1.

The above criteria do not rely on particular assumptions about the mass range where the Higgs bosons are searched; event-shape variables (like thrust and Fox-Wolfram momenta) commonly used in the DELPHI SM and MSSM Higgs analyses are left out of this search because they are not adapted to searches for Higgs bosons near the  $b\bar{b}$  threshold.

The number of selected events in each analysis is shown in table 1, together with expected background and signal efficiencies. The 2b-Z analysis has also been applied to the  $h_i A_j$  channel, and is used in cases where both processes are present. The  $m_Z$  constraint is of course not adapted to  $h_i A_j$  pair production, but on the other hand the efficiency of tagging two b-quarks is higher than in the  $h_i Z$  channel due to the presence of four b-quarks, and in total the obtained efficiency remains reasonable. The pairing is for the same reason essentially determined by the  $m_Z$  constraint, and it appears that a combination with a dijet of mass reasonably close to  $m_Z$  is often found. The mirror analysis, consisting of applying the 4b analysis to the  $h_i Z$  channel, gives much worse results.

At this level of selection, the number of expected signal and background events are comparable. The simulation of background and signal processes is described in [10]. The composition of the expected background in the  $h_i A_j$  case is roughly 50%  $e^+e^- \rightarrow b\bar{b}$  with hard gluon radiation and frequent gluon splitting into  $b\bar{b}$  or  $c\bar{c}$ , and 50%  $e^+e^- \rightarrow ZZ$  with mainly  $Z \rightarrow b\bar{b}$ . In the  $h_i Z$  case, the expected background is much higher from both sources, since only two b-quarks are required in the final state and the background rejection power is lower.

The efficiencies on  $h_i A_j$  and  $h_i Z$  signals are verified to be independent of the simulated Higgs boson masses within errors, for the Higgs boson mass range of [10], and are given averaged over all simulated mass points. Consequently, although the analyses given here are less performant than analyses dedicated to heavy Higgs bosons as is the case in Standard Model and MSSM searches, their kinematic domain of validity is much enhanced.



We want to stress here that no signal has however been simulated with Higgs boson masses very close to the  $b\bar{b}$  threshold yet, so that efficiencies in this range remain to be checked; our analysis assumes that the decay products of the Higgs bosons are always resolved as two jets. This point is particularly important in the  $h_i A_j$  channel, for which the simulation has been done in the framework of the MSSM, where the  $h$  and  $A$  masses are typically of same order. In our situation, their mass difference can be arbitrary and it is not certain that in extreme cases the  $2b$ - $Z$  efficiencies remain at the same level.

The values of table 1 assume only standard decays of all Higgs bosons. In particular, the cascade  $h \rightarrow AA$  followed by  $A \rightarrow b\bar{b}$  is not specifically looked at, although it is often kinematically allowed in this model. However, since the only effect of this cascade as far as our analysis is concerned is to increase the  $b$ -content of the signal (we recall that we only consider cases where all Higgs bosons have mass larger than  $12 \text{ GeV}/c^2$ ), the sensitivity to these decays is underestimated and the efficiencies of table 1 can safely be used.

## 4 Interpretation

The interpretation of the results will be given in the  $m'_A$ - $\tan\beta$  plane, familiar from the MSSM, for fixed values of  $\lambda$ . We always place ourselves in the worst-case of radiative corrections, obtained for maximal mixing in the stop sector. All other parameters appearing in the corrections are taken identical to their values in the so-called MSSM benchmark scan [10].

Signal efficiencies, expected background rate and observed data are taken from the analyses described in the previous paragraph for the  $h_i A_j$  and  $h_i Z$  searches. In addition, we will use the latest published LEP limits on the charged Higgs bosons mass [15], which imply  $m_{H^\pm} > 69 \text{ GeV}/c^2$ .

A scan of the parameter space of the model can now be performed. For each point in the  $m'_A$ - $\tan\beta$  plane, and with fixed  $\lambda$ , the charged Higgs bosons mass as well as the upper  $2 \times 2$  blocks of the Higgs mass matrices are determined. Five parameters remain unknown, controlling singlet mixing in the CP-even and odd sectors. We choose the parameterization discussed in section 2; namely, we scan over the mass of the lightest CP-odd Higgs boson,  $m_{A_1}$ , the CP-odd mixing angle  $\gamma$ , the mass of the lightest CP-even Higgs boson  $m_{h_1}$ , its  $R$ -factor, and one CP-even mixing angle. For every configuration of these parameters, all masses and  $R$  coupling factors are determined by numerical diagonalization of the mass matrices. We then compute all  $h_i Z$  and  $h_i A_j$  cross-sections (we use the implementation of [16], together with the  $R$  suppression factors), and all  $h_i$  and  $A_j$  branching fractions (using [17]).

At high values of  $\tan\beta$ , the  $h_i A_j$  processes dominate, whereas at low values, the  $h_i Z$  couplings are important. In both cases, the corresponding efficiencies obtained previously are applied to the sum of the individual cross-sections to obtain the total number of expected events, and we compare with data. For intermediate values, where  $h_i A_j$  and  $h_i Z$  coexist, the  $h_i Z$  analysis is applied to all signals. A given singlet mixing configuration is considered excluded if the data disfavour it with a confidence of at least 95%; an  $m'_A$ - $\tan\beta$  point is excluded if all corresponding singlet mixing cases are excluded.

The regions covered by the various searches are illustrated in figure 2 by dashed ( $\lambda=0$ ) and full lines ( $\lambda=0.6$ ). To study the dependence on  $\lambda$ , singlet mixing is turned off for

simplicity. The  $h_i Z$  processes only contribute at small values of  $\lambda$ . This can be understood looking at Eq.5: in this model, small values of  $\tan \beta$  do not imply a light Higgs boson, and the  $h_i Z$  processes can be kinematically forbidden. The contribution of the  $h_i A_j$  channels however increases with  $\lambda$  in this region. To see this, one can assume no singlet mixing in the CP-even sector:  $M_{even}^2$  then reduces to its upper  $2 \times 2$  block which is identical to the MSSM CP-even mass matrix, except for the off-diagonal terms involving  $\lambda$ . If, at  $\lambda=0$ , this matrix is diagonalized by a rotation of angle  $\alpha$  satisfying  $\cos^2(\beta - \alpha) \sim 0$  with zero  $h_i A_j$  couplings, then changing the value of  $\lambda$  will imply  $\cos^2(\beta - \alpha) > 0$  and the couplings switch on. Similarly, the results are independent of  $\lambda$  at large  $\tan \beta$ , because the off diagonal terms of  $M_{even}^2$  are proportional to  $c_\beta s_\beta$ , which goes to 0 in this limit.

Searches for charged Higgs boson mass play an important role when  $\lambda > 0$ . Almost independently of  $\tan \beta$  (the residual dependence at high values of  $\tan \beta$  comes from the radiative corrections), the LEP2 limit allows to test  $m'_A$  up to  $95 \text{ GeV}/c^2$  when  $\lambda$  is at its maximal value.

One finds in general that when  $\tan \beta$  is small, the increase with  $\lambda$  of the  $h_i A_j$  cross-sections and the opening of  $H^+ H^-$  overcompensates the loss of sensitivity from  $h_i Z$ . Consequently, the most difficult case is found at  $\lambda = 0$ . Results in this limit are displayed in figure 3, where the effect of singlet mixing has been taken into account. Results obtained in the limit of singlet decoupling, leading to an effective MSSM, are also recalled. For  $\tan \beta > 1$ , the lowest limit is found in the region where  $h_i Z$  and  $h_i A_j$  coexist, and is:

$$m'_A > 69 \text{ GeV}/c^2 . \quad (8)$$

At high values of  $\tan \beta$ , one finds  $m'_A > 72 \text{ GeV}/c^2$ , and for  $\tan \beta < 1$  no limit can be set.

## 5 Conclusions

We presented a framework for testing a non minimal supersymmetric model, containing an additional gauge-singlet Higgs field. The effect of this extension is to largely release the constraints on Higgs boson masses and couplings that are typical to the MSSM. Searches have been performed assuming that all Higgs bosons are heavy enough to decay into a  $b\bar{b}$  pair. Under this assumption,  $\tan \beta$ -dependent limits on the CP-odd mass parameter  $m'_A$  have been found. A complete exploration of the model however requires searches for final states arising from lighter Higgs boson decays.

The authors of [3] have found very poor prospects for the discovery of the Higgs bosons of this model, with respect to the MSSM, due to the possibility of very weakly coupled Higgs bosons. The exclusion potential of LEP2 is however still reasonable since the large number of processes compensates for the weakened production rates.

## Acknowledgments

We are grateful to S. King and P. White for discussions, and for making their implementation of radiative corrections in this model available to us.

## References

- [1] ALEPH Collaboration, ALEPH 99-007 CONF 99-003  
DELPHI Collaboration, DELPHI 99-8 MORIO CONF 208  
L3 Collaboration, L3 2383  
OPAL Collaboration, OPAL PN382
- [2] DELPHI Collaboration, DELPHI note 98-117 ICHEP'98 CONF 179
- [3] S.F. King, P.L. White, Phys. Rev. **D53**, 4049 (1996)
- [4] P. Fayet, Nucl. Phys. **B90**, 104 (1975)
- [5] A discussion of the NMSSM as a possible solution to the  $\mu$ -problem, and of the new questions it raises, is for instance in:  
S.A. Abel, S.Sarkar, P.L. White, Nucl. Phys. **B454**, 663 (1995)
- [6] M. Drees, Int. J. Mod. Phys. **A4**, 3635 (1989)
- [7] J. Ellis, J.F. Gunion, H.E. Haber, L. Roszkowski, F. Zwirner, Phys. Rev. **D39**, 844 (1989)
- [8] M. Carena, J. Espinosa, M. Quiros, C. Wagner, Phys. Lett. **B355**, 209 (1995)
- [9] P. Lutz, G. Piana, F. Richard, V. Ruhlmann, G. Wormser, DELPHI note 92-80 Dallas PHYS 191
- [10] DELPHI Collaboration, CERN-EP 99-006
- [11] M. Boonekamp, PhD thesis, may 1999, DAPNIA report DAPNIA/SPP 99-1001
- [12] S. Catani, Yu.L. Dokshitzer, M. Olson, G. Turnock, B.R. Webber, Phys. Lett. **B269**, 432 (1991)
- [13] G. Borisov, Nucl. Instr. Meth. **A417**, 384 (1998); M. Boonekamp, DELPHI note 98-54 PHYS 779
- [14] DELPHI Collaboration, E. Phys. J. **C2**, 581 (1998)
- [15] ALEPH, DELPHI, L3, OPAL Collaborations, CERN-EP 99-060
- [16] E. Gross, B.A. Kniehl, G. Wolf, Zeit. Phys. **C63**, 427 (1994); err. ibid. **C66**, 32 (1995)
- [17] A. Djouadi, J. Kalinowski, M. Spira, Comput. Phys. Commun. **108**, 56 (1998)

# DELPHI Preliminary

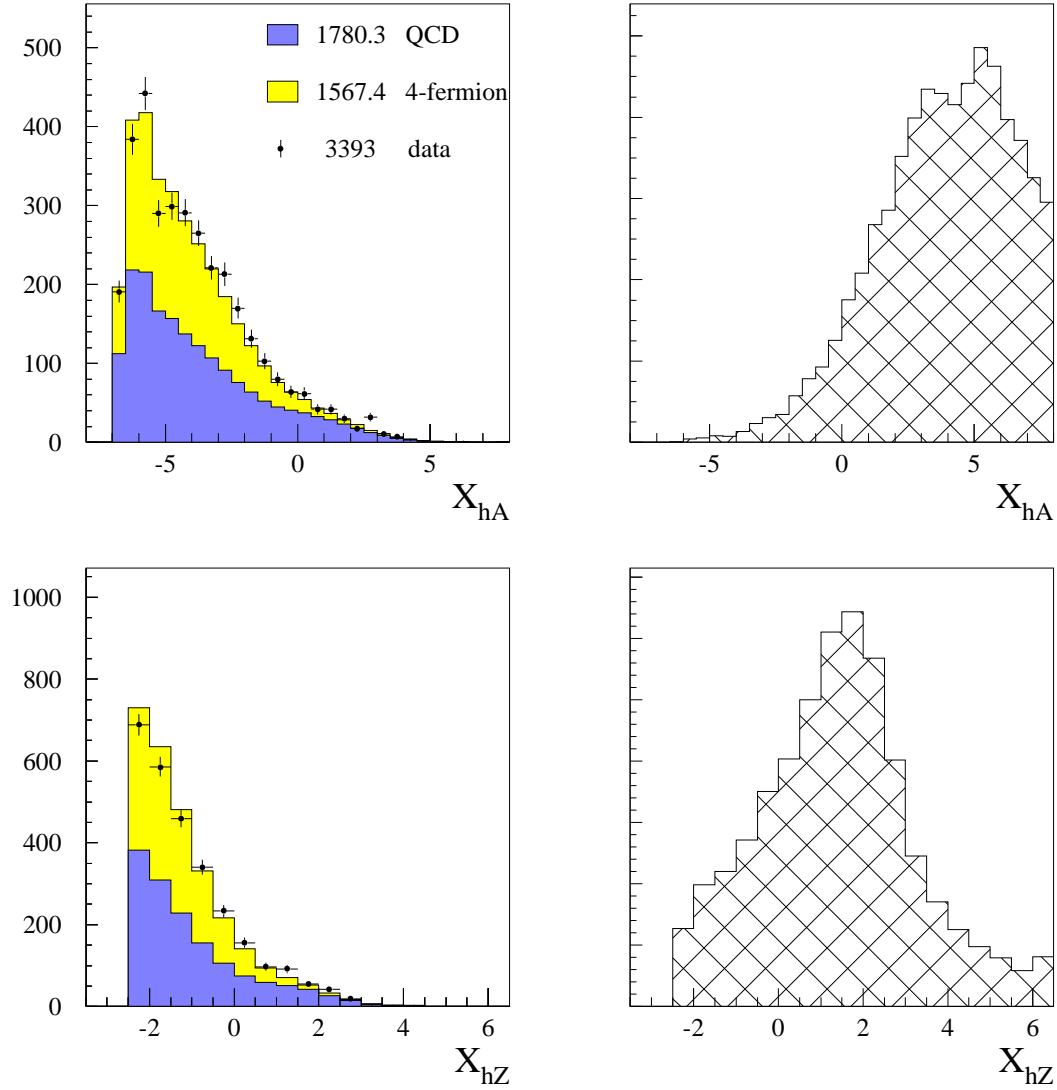


Figure 1: Distributions of the discriminating variables  $X_{hA}$ ,  $X_{hZ}$ , after the preselection step. The data and expected background are shown on the left. The signal is shown in the upper right ( $h_i A_j$ ) and lower right ( $h_i Z$ ) figures.

## DELPHI Preliminary

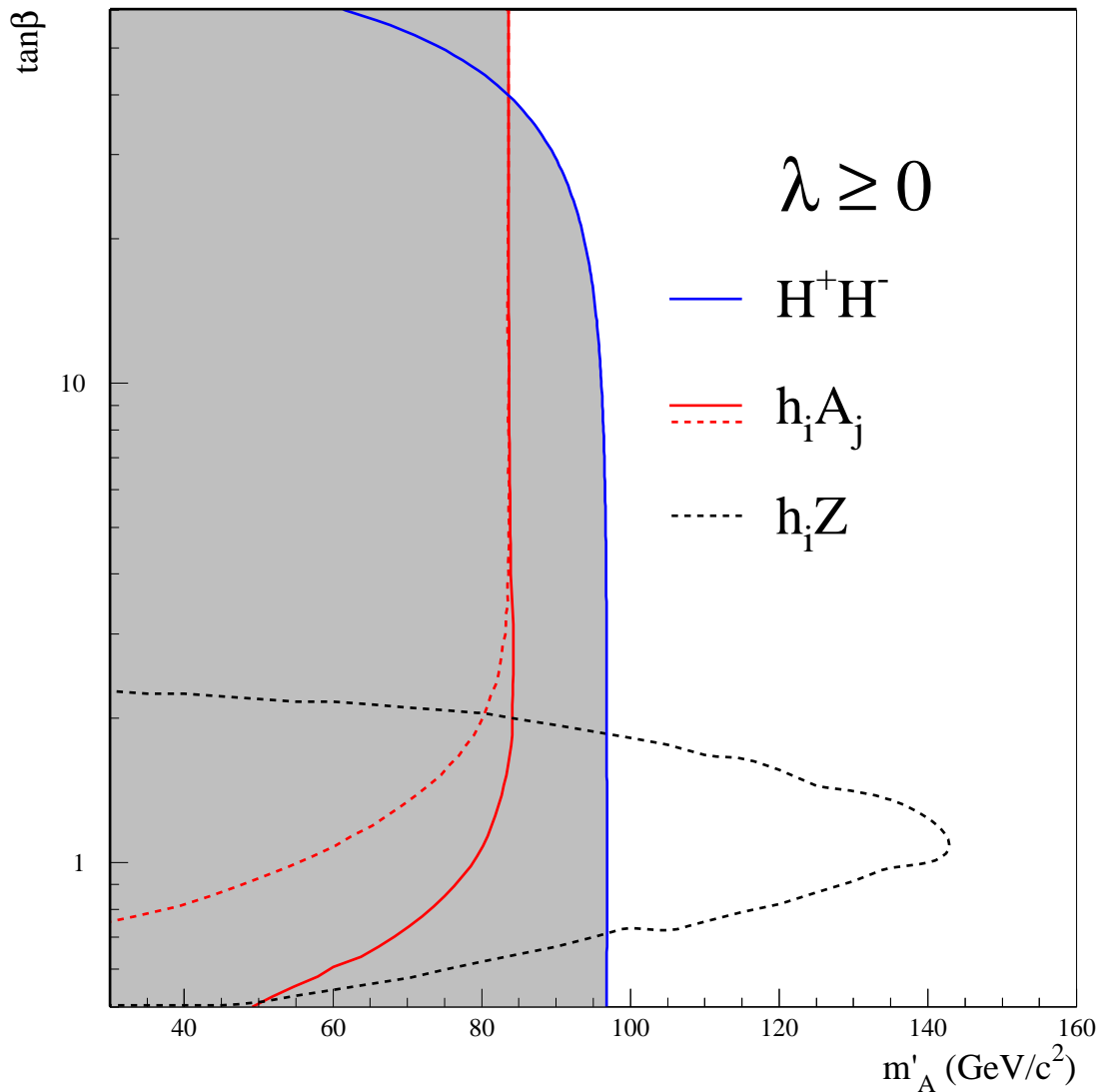


Figure 2: Excluded regions in the general MSSM plus a singlet, for two extreme values of  $\lambda$ . For all channels, the  $\lambda = 0$  case is illustrated by dashed lines, and full lines represent the  $\lambda = 0.6$  case. No singlet mixing was assumed. The  $h_i Z$  channel contributes only at  $\lambda = 0$  in this figure, while the charged Higgs boson searches contribute at  $\lambda = 0.6$ . The  $h_i A_j$  channel contribution is independent of  $\lambda$  at high  $\tan \beta$ , and increases with  $\lambda$  at low  $\tan \beta$ .

## DELPHI Preliminary

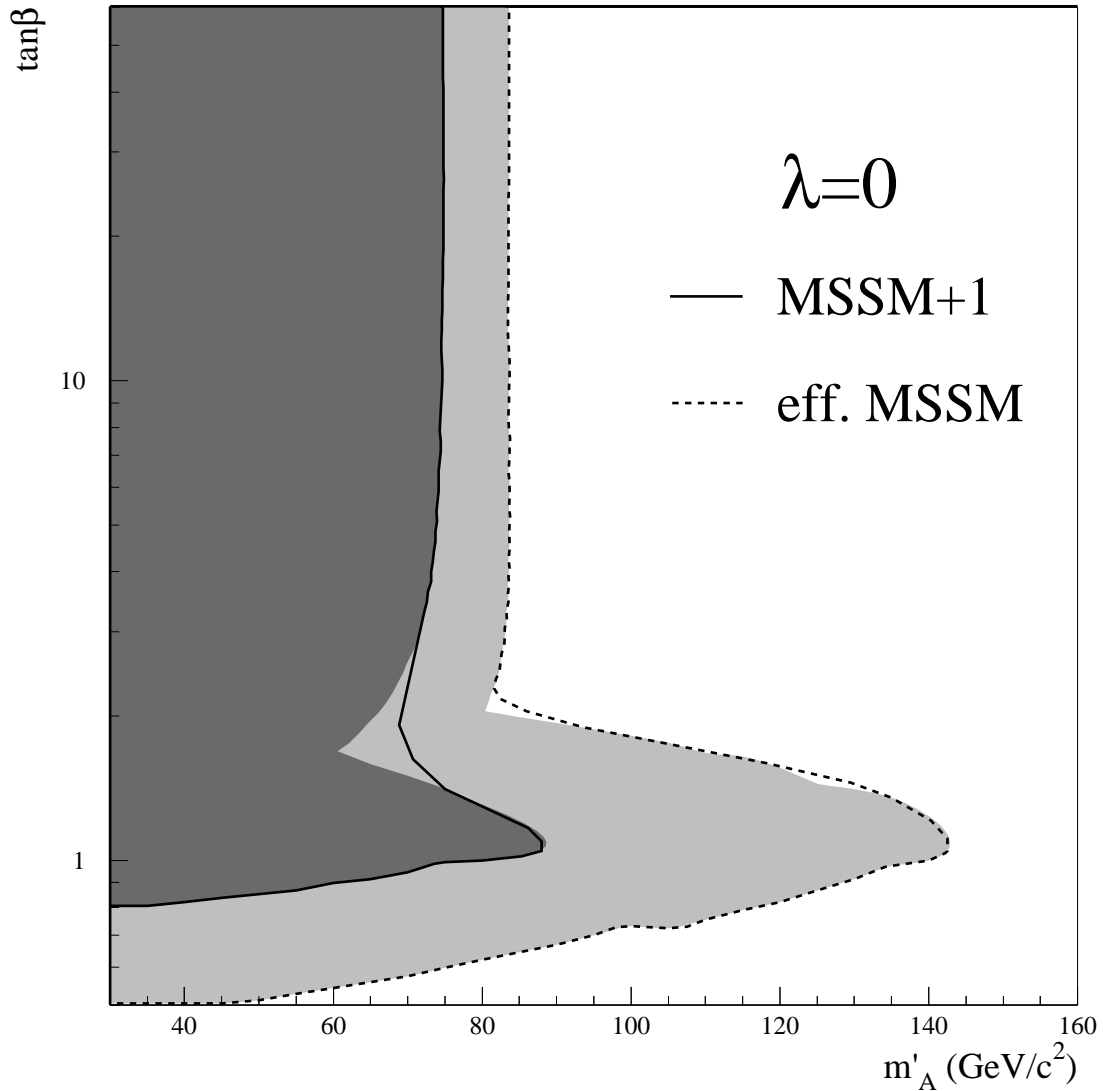


Figure 3: Excluded regions in the general MSSM plus a singlet, at  $\lambda = 0$ , by the two-channel search described in the text : the dashed line assumes no singlet mixing, corresponding to an effective MSSM, while the full line includes this effect. The shaded regions correspond in both cases to the sum of the regions excluded by the  $h_i A_j$  and  $h_i Z$  single-channel searches.